Interaction of Multiple Drops and Formation of Toroidal-Spiral Particles
SUPPLEMENTAL MATERIAL

Paola Leon Plata, Ying Liu,* and Ludwig C. Nitsche

Department of Chemical Engineering, University of Illinois at Chicago,
810 South Clintoin Street, Chicago, IL 60607, USA.

I. EXPERIMENTAL DETAILS

Each polymer drop phase was pumped through a syringe affixed to a single or multi-capillary assembly (glass capillaries embedded into polyurethane tubing (ID: 2.4mm, OD: 4.0mm) to generate the central (main) and surrounding drops respectively. The volume and infuse rate of each syringe was controlled individually by a set of two syringe pumps (PHD 2000 programmable, Harvard Apparatus, Hollistom, MA). Three glass capillaries (ID: 536.2 μm, OD: 658.3 μm, Polymicro Technologies) were fixed to a triangular geometry that neighbored equidistantly the central one. All capillaries were submerged into the bulk solution (63wt% glycerol and 37wt% EtOH). In order to achieve simultaneous drop fall and better control entrapment, the surrounding capillaries were optimized to be at a distance of 3 mm to the center one and with a height difference (tip to tip) of about 2 mm. The target volume for each polymer phase is infused by separate syringe pump and ranged between 30-40 μl, whereas the surrounding drops 20-10 μl. Thus, the infused volume for each surrounding drop varied from 3.3 to 6.6 μl. The flow rate was set to be low to attain comparable (i.e., low) Reynolds number to the simulations and in such a way that both drops will be completely infused at the same time. This ranged from 1 to 1.2 ml/min and 0.3 to 0.35 ml/min for central and surrounding drops respectively. The corresponding dimensionless (spherical) radius of the surrounding drops could vary from 0.60 to 0.44, when experimental capillary distance ($d_{1\alpha}$) is around 3 mm.

II. RELATIONSHIP BETWEEN TIME VARIABLES IN THE EXPERIMENTS VERSUS SIMULATIONS

At each time point in the experiment ("experimental time") the cumulative distance of sedimentation Z was read off from the ruled scale in the background of the frame and reduced by the horizontally projected radius of the drop R_1 in the starting frame. For the corresponding reduced distance Z/R_1 in the simulation, the "simulation time" could be determined. The two times are plotted against each other in Figure SM1 and show an essentially perfectly linear relationship.

III. REYNOLDS NUMBER IN THE EXPERIMENTS

For sedimentation of the main polymeric drop, the Reynolds number is calculated from the expression $Re = UR/\nu$, where U (m/s) and R (m) correspond to the sedimentation velocity and radius of the main polymer drop (at the initial stage) and ν (m^2/s) to the kinematic viscosity of the surrounding bath solution. Drop radius is measured at initial stage and distance travelled (by the bottom of the drop) is measured at specific frames captured by the camera, where time is obtained from the camera recording speed. Then a finite-difference of distance travelled as a function of time is used to approximate the average sedimentation velocity. The range of Re for single-drop and four-drop sedimentation are given in Figs. 2 and 3; these are below 0.1. The HR solution given as in Eq. (5) for a spherical drop of volume-equivalent radius of the total volume infused (40 μl) is calculated as $Re = 0.0064$.

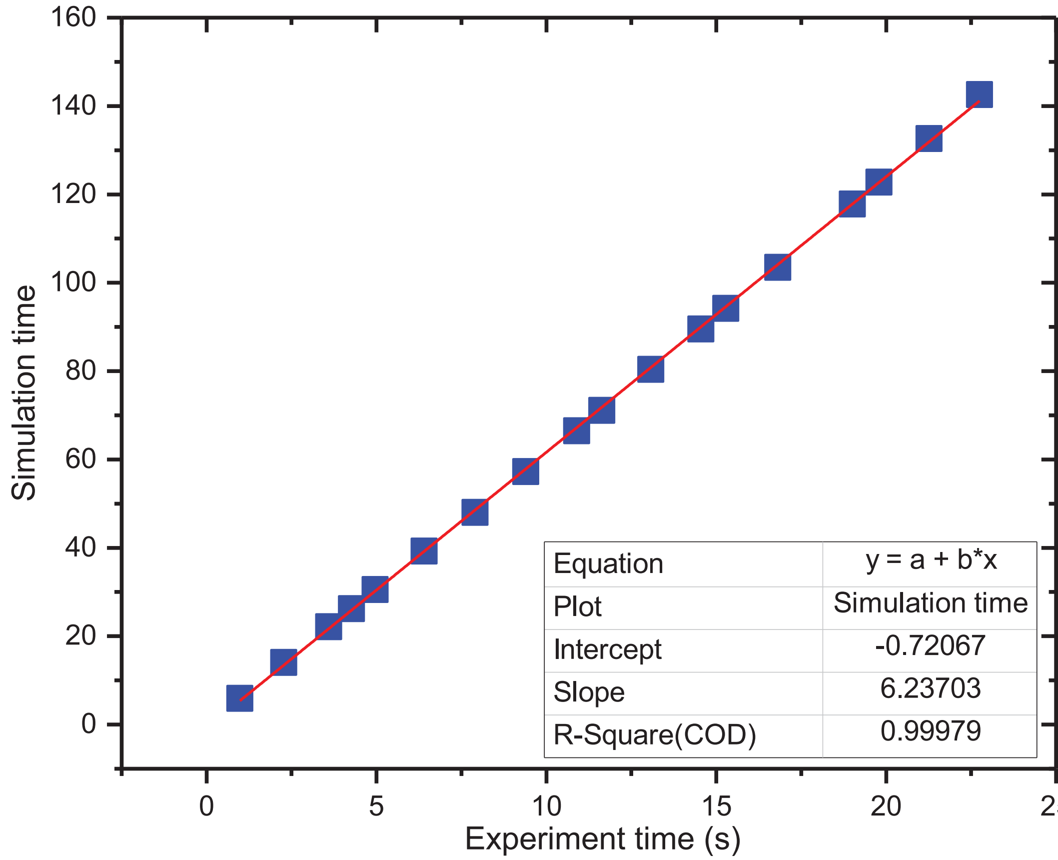

FIG. I. Linear relation between experimental time and simulated (dimensionless) time, once reduced vertical position (Z/R_1) of the bottom of a single drop (Fig. 2) has been matched at each time point.

IV. ESTIMATES OF DROP VOLUMES BASED ON LABORATORY IMAGES

Table SM1 provides an estimates of the reduced volume of the main drop at various time points, including that image (marked with an asterisk $*$) used to start the simulations in Fig. 2(a), 3(a) or 4(b). The raw volumes are based upon the image conversion algorithm. They represent slight overestimates because this methodology does not account for the circumferential depressions marked with arrows in Figs. 2(a), 3(a) and 4(b). The excess volume to be subtracted off is here estimated using half of an elliptic torus that is heuristically fitted to the profile of the depression. In the last column, corrected volumes at each time point are compared with the volume for the starting configuration, to ascertain any injection still in progress.

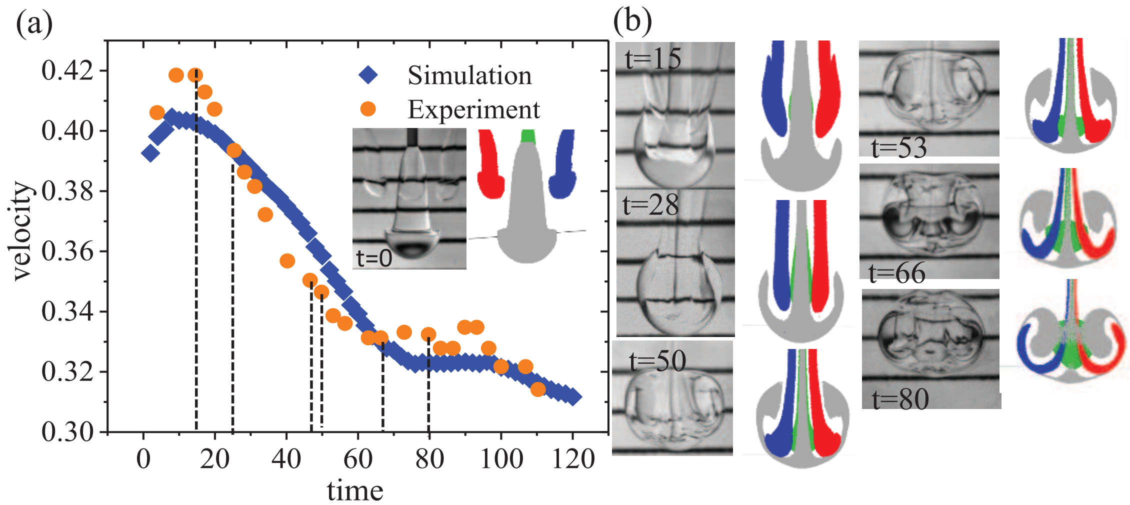

FIG. II. Counterpart of Fig. 3 for a nominally identical experiment and computer simulation based upon the corresponding, numerically converted initial configuration. Comparing the two sets of images indicates the level of reproducibility that is achievable. Please refer to the caption of Fig. 3 for descriptions.

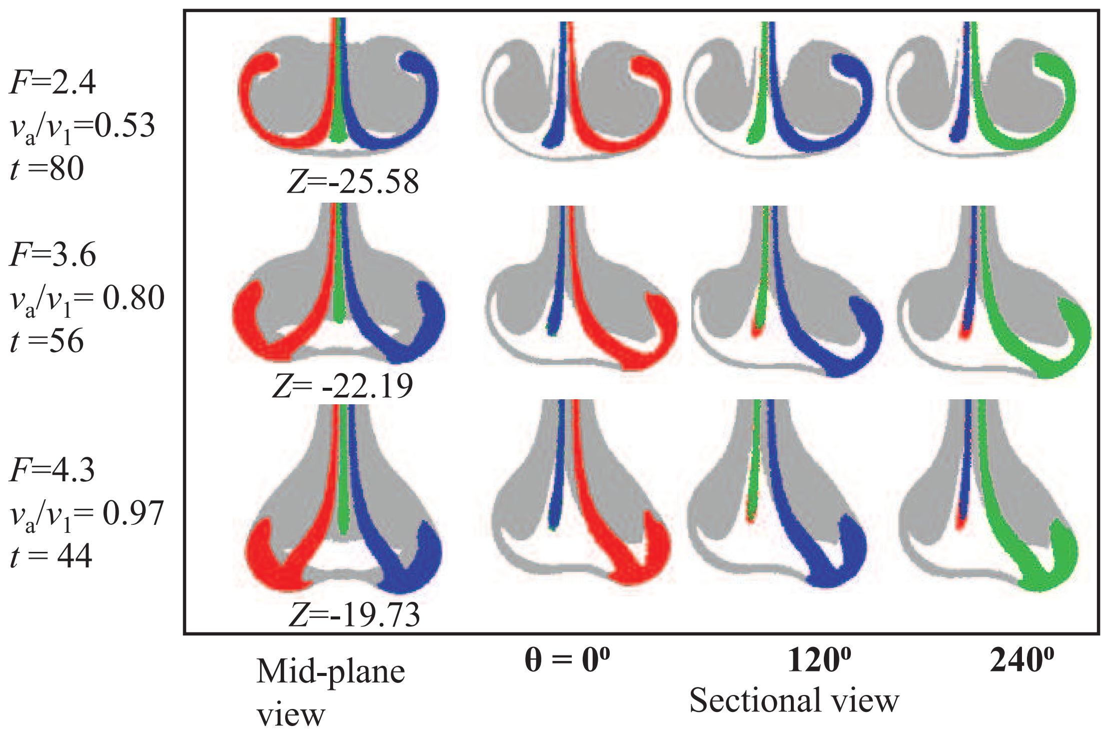

FIG. III. Counterpart of Fig. 5 when all satellite drops have the same radii and force densities. Comparison with the images Fig. 5 indicates how different sizes of satellite drops result in more asymmetric TS shapes.

TABLE I. Estimate of the reduced volume of the main drop at various time points.

Figure	Lab time t (s)	Raw dimensionless volume before correction	Volume correction (elliptic torus)	Volume correction (percent)	Corrected volume	Difference in volume compared to starting configuration
2(a)	2.312*	13.77	0.264	1.91%	13.50	–
3(a)	2.298*	13.24	0.26	1.93%	12.98	–
	3.124	18.04	0.44	2.43%	17.73	+36.5%
4(a)	1.607	18.17	0.34	1.9%	17.83	-21.9%
	2.012	23.49	1.12	4.8%	22.37	-2.1%
	2.147*	24.16	1.32	5.5%	22.84	–
	2.613	27.34	2.71	9.9%	24.63	+7.8%
	2.793	28.09	3.26	11.6%	24.84	+8.7%

V. EFFECT OF VISCOSITY RATIO UPON FORMATION OF THE TS CHANNEL

As a crude approximation, we shall here asertain whether the HR solution for a volume-equivalent sphere can reveal something about effect of viscosity ratio $\lambda = \mu_{\rm drop}/\mu_{\rm bath}$ upon the dynamics of formation of the TS channel. For a given streamline in the toroidal vortex of a sedimenting sphere, the time $T(\lambda)$ required to complete one circuit in a meridian plane of the HR solution may roughly indicate the rate at which the advancing tip of the TS channel winds around. This circulation time itself varies with the streamline, but the time ratio turns out to be the same for all streamlines:

$$T(\lambda)/T(1) \ = \ 1 + (\lambda - 1)/2$$

Higher (lower) viscosity of the drop compared with the surrounding bath means a slower (faster) vortex. At the dimensionless time point $t = 104.1$ in Fig. 2(b), the drop has descended by 25.81 units and the simulated TS channel (with $\lambda = 1$) has made roughly a complete turn, whereas in the experimental image the TS channel has wound further around by approximately a quarter turn. The spherical HR approximation would imply significantly lower viscosity of the drop in the experiments ($\lambda = 0.6$). This is an underestimate of the actual drop viscosity: $\mu_{\rm drop} = 0.057$ Pa·s and $\lambda = 0.904$. While the HR sedimentation velocity of 0.29 is quite close to that for the bell-shaped drop (Fig. 2(a)), the rate of circulation of the spherical vortex is 3 to 4 times higher and does not do a good job of representing TS channel winding around. The shape of the drop seems to have a strong effect: this will be the focus of future numerical work on non-unit viscosity ratios.